Biochimica et Biophysica Acta 1808 (2011) 706–716

Contents lists available at ScienceDirect

Biochimica et Biophysica Acta

journal homepage: www.elsevier.com/locate/bbamem

High water solubility and fold in amphipols of proteins with large hydrophobic regions: Oleosins and caleosin from seed lipid bodies

Yann Gohon [a], Jean-David Vindigni [a], Agnès Pallier [b], Frank Wien [c], Hervé Celia [d], Alexandre Giuliani [c,e], Christophe Tribet [b,1], Thierry Chardot [a], Pierre Briozzo [a,*]

[a] INRA, AgroParisTech, UMR 1318 Institut Jean-Pierre Bourgin, Dynamic and Structure of Lipid Bodies, F-78850 Thiverval Grignon, France
[b] ESPCI, UMR CNRS 7615, Physico-Chimie des Polymères et des Milieux Dispersés, 10 rue Vauquelin, F-75005 Paris, France
[c] Synchrotron Soleil, Saint-Aubin, F-91192 Gif-sur-Yvette, France
[d] IBSM-LISM, UPR 9027 CNRS, 31 Chemin Joseph Aiguier, F-13402 Marseille, France
[e] CEPIA, INRA, BP 71627, F-44316 Nantes Cedex 3, France

ARTICLE INFO

Article history:
Received 14 July 2010
Received in revised form 12 November 2010
Accepted 3 December 2010
Available online 10 December 2010

Keywords:
Lipid body
Oleosin
Caleosin
Amphiphilic polymer
Secondary structure

ABSTRACT

Seed lipid bodies constitute natural emulsions stabilized by specialized integral membrane proteins, among which the most abundant are oleosins, followed by the calcium binding caleosin. These proteins exhibit a triblock structure, with a highly hydrophobic central region comprising up to 71 residues. Little is known on their three-dimensional structure. Here we report the solubilization of caleosin and of two oleosins in aqueous solution, using various detergents or original amphiphilic polymers, amphipols. All three proteins, insoluble in water buffers, were maintained soluble either by anionic detergents or amphipols. Neutral detergents were ineffective. In complex with amphipols the oleosins and caleosin contain more beta and less alpha secondary structures than in the SDS detergent, as evaluated by synchrotron radiation circular dichroism. These are the first reported structural results on lipid bodies proteins maintained in solution with amphipols, a promising alternative to notoriously denaturing detergents.

1. Introduction

Highly hydrophobic proteins, including integral membrane proteins (IMPs) are prone to severe aggregation in water. Their handling in aqueous solution is a critical issue, not only in fundamental biochemistry research, but also from a practical perspective. IMPs inserted in the cell membrane phospholipid bilayer are the targets of the majority of commercialized drugs [1]. Besides, structural membrane proteins found in the phospholipid monolayer of lipid storage organelles (lipid bodies: LBs, also called oil bodies, lipid droplets or oleosomes) are also related to health issues. Human low density lipoproteins are associated with coronary heart disease risk and seed oil body proteins to allergies [2]. Due to their role in organelles stabilization, the latter proteins have an important impact on oil extraction from seed LBs of economically important oleaginous plants (rapeseed, soy, sesame…).

In oleaginous plants, neutral lipids are stored into specialized organelles, with diameter ranging from 0.2 to 3 μm. These LBs represent the source of energy for seeds. Plant LB proteins fall into two types: i) structural proteins, the most abundant, mainly represented by oleosins. In *Arabidopsis thaliana*, five seed-specific oleosins (S1 to S5) with molecular mass comprised between 14 and 21 kDa have been detected [3]; ii) minor proteins such as caleosin, a calcium binding protein [4], stereoleosin, an enzyme using hydroxysteroids as substrates *in vitro* [5] and lipases [6]. LB integral proteins are important in seed tissue for controlling oil body structure and lipid accumulation [7]. Thus, oleosomes remain small in size, allowing a quick mobilization of lipids for germination, a period of active metabolism.

The organization of IMPs inserted into a monolayer of phospholipids is poorly known. Thus, few data concern the structure of oleosins, even less data being available for caleosin. Caleosin and oleosins, despite low sequence identity (26%), share a similar amphiphilic triblock architecture. The central region is highly hydrophobic. In the case of oleosins it is the longest hydrophobic region (71 residues for the two oleosins studied in this work, S3 and S5) known to occur in natural proteins. This is in accordance with its insertion into a phospholipid monolayer, and probably into the lipid core packed by this monolayer. This central region comprises three conserved prolines forming a characteristic proline knot motif, which is involved in protein targeting to lipid bodies, and is flanked with polar N- and C-termini of variable lengths [8]. Upon calcium binding, the lipid bodies' interfacial behaviour as well as caleosin's interfacial properties are strongly modified [9], making caleosin an interesting target for understanding lipid bodies stability. Caleosin central hydrophobic region is significantly shorter (41 residues) than

* Corresponding author. Dynamic and Structure of Lipid Bodies, UMR INRA-AgroParisTech 1318, Institut Jean-Pierre Bourgin, AgroParisTech, F-78850 Thiverval Grignon, France. Tel.: +33 1 30 81 54 73; fax: +33 1 30 81 53 73.
E-mail address: pierre.briozzo@grignon.inra.fr (P. Briozzo).
[1] Present address: Ecole Normale Supérieure, UMR 8640 CNRS-ENS-UPMC, Département de Chimie, 24 rue Lhomond, F-75005 Paris, France.

0005-2736/$ – see front matter © 2010 Elsevier B.V. All rights reserved.
doi:10.1016/j.bbamem.2010.12.002

that from oleosins, which makes caleosin (MW 28 kDa) a more hydrophilic protein. Oleosin S5 is the shortest member (14.9 kDa) of the oleosin family, due to shorter N and C termini. It is therefore the most hydrophobic oleosin. Oleosin S3 (18.6 kDa), the most abundant oleosin in *A. thaliana* seeds, with N- and C-termini longer than those of S5, is less hydrophobic. S3 and S5 share 63% sequence identity. There are very few solved high-resolution structures of full-length integral proteins from LBs. They mainly belong to apolipoproteins (for instance human apo A-I [10] or locust apolipophorin 3 [11]). For triblock IMPs from lipid bodies, there is no known high-resolution structure yet.

The difficulty in handling and purifying IMPs derives directly from their amphiphilic structures, which display regions adapted to interact with the lipid membrane and other regions protruding toward the aqueous media. In order to achieve structural studies of such proteins, IMPs have to be solubilized in aqueous solutions in conditions that prevent aggregation between their hydrophobic regions. This has been traditionally achieved by using small molecular surfactants added in a concentration close to their critical micellar concentration (CMC). These surfactants (called detergents) cooperatively assemble on the hydrophobic regions of the proteins, maintaining solubility as long as the total detergent concentration is higher than its CMC. However, the dilution of the detergent below its CMC usually triggers the aggregation of the IMPs, whereas high detergent concentrations may denature the proteins. In addition, the radius of detergents micelles is matching with the height of transmembrane domains from the plasma membrane proteins, but might be less adapted to protect longer hydrophobic domains like those of oleosins and caleosin that probably protrudes into the lipid core of the LBs.

Different authors extracted oleosins and caleosin from seeds with organic solvents [12] or tried to solubilize their recombinant forms using alcohols [13], urea [14] or SDS [15], and recently various detergents [16]. However, none of these authors used stringent enough criteria to measure solubility, centrifugation when used being far below the conditions used in the present study (200 000 *g* ultracentrifugation). The use of milder detergents or polymeric amphiphiles called amphipols [17] is expected to provide better conditions for structural studies.

Amphipols (APols), like detergents, protect the hydrophobic domains of IMPs from contact with water. These polymeric surfactants can maintain soluble most membrane proteins found in phospholipids bilayers [18], irrespective of their secondary structure. When APols are used instead of detergents, the stability upon the dilution of transmembrane proteins/amphiphile complexes is significantly enhanced [19]. So far, APols have not been assayed with IMPs from the lipid bodies. Conventional APols have a random distribution of octyl hydrophobes in their chain. As molecular detergents, they form micelles with radii typically below 5 nm. In this study, we used three polymers (quoted A8-35R, A12-60R and A12-80R: R stands for random) as representative of random APols (Fig. 1, and Table 1). In addition, we considered other APols that assemble in larger assemblies. The integration level of octyl hydrophobes in these original polymers (quoted A12-80B, A12-80B1 and A12-80B2: B for blocky) is essentially the same as in A8-35R, but their distribution in the chain is multiblock instead of random [20]. We studied the efficiency of these polymers and detergents (either charged or neutral) to solubilize caleosin and S5 oleosin. The size of APols, protein/APol, and protein/detergent complexes were characterized by X-ray and light scattering. Secondary structure content of LB proteins in different surfactant environments was determined by synchrotron radiation circular dichroism (SRCD).

2. Materials and methods

2.1. Amphipol synthesis

Conventional amphipols (APols) are typically obtained by radical copolymerization of hydrophilic and hydrophobic monomers [21], or modification of commercially available hydrophilic parent chain [22], which is a poly(acrylic) acid in the case of the most popular APol A8-35R. Both approaches result in macromolecules with relatively high dispersity in length (polydispersity index Ip ~1.7) and statistic distributions of hydrophobes. To obtain APols with lower dispersity, we synthesized a parent poly(ter-butyl methacrylate) by controlled radical polymerization (atom transfer radical polymerization ATRP, Ip<1.2) as described in Ref. [20]. Following extensive acidolysis, the parent chain was post-modified by coupling with octylamine either in homogeneous solution of N-methylpyrrolidone (to obtain random copolymers) or in aqueous micellar solution (yielding blocky polymers). Polyacrylic acids with low (home made) and high Ip (Sigma chem., Mw 5000 g/mol, Ip ~1.7) were modified by the same procedure. In the case of blocky polymers, modifications were carried out in micellar solutions of sodium dodecyl sulfate (SDS) [20]. SDS was removed by precipitation in 1 M KCl and dialysis against water (Spectrapor membranes, Slide-A-Lyzer, MWCO 3500). The presence of residual SDS was detected by NMR in some samples, even after 2-day long dialysis of the polymer against water. We checked that the SDS in polymer solution did not modify by more than 10% the radii and MW of polymer self-assemblies [20]. We used only those samples with the lowest SDS:polymer fraction (≤0.06 g/g). The maximal residual SDS amount found in blocky APols (0.06 g/g) is not responsible for protein solubilization: as an example, 1 g A12-80B1/g Clo results in 78% Clo solubilization; this corresponds to 0.06 g SDS/g Clo, which accounts for only 12% solubilization (Fig. 3 A and B). The composition and structural parameters of polymers are given in Table 1. A12-60R, A12-80R, A12-80B, A12-80B1 and A12-80B2 contain a similar average density of octylacrylamide as A8-35R. They differ from A8-35R in that they contain a sodium methacrylate hydrophilic moiety instead of sodium acrylate, and no isopropyl side groups (Fig. 1). Modification of the parent chain in homogeneous conditions yielded random copolymers similar to the most used APol A8-35R (a random terpolymer of octylacrylamide, isopropylacrylamide and sodium acrylate); modification in micellar aqueous dispersion yielded multi-blocky distributions of the hydrophobes.

2.2. Transmission electron microscopy (TEM) and Cryo-TEM on amphipols

Cryo-TEM experiments were carried out on a FEI CM120 electron microscope equipped with a LaB6 filament and operating at 100 kV.

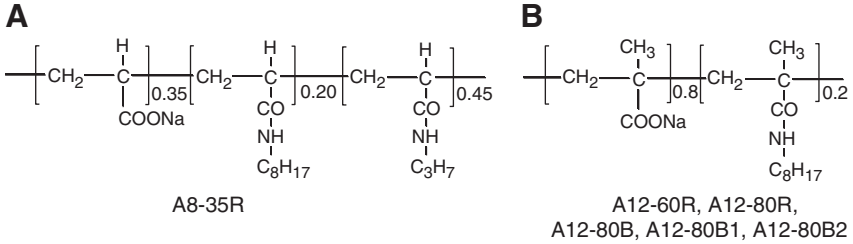

Fig. 1. Chemical structure of amphipols used in this study. (A) Polyacrylate-based polymer A8-35R, random distribution of side chains. (B) Polymethacrylate-based polymers with random (A12-60R and A12-80R) or blocky (A12-80B, A12-80B1, and A12-80B2) distribution of side chains. Molar fraction distribution is indicated in lower case.

Table 1
Chemical and physical characteristics of amphipols used in this study.

Name used in this study	Chemical name	Laboratory name	Polymer of	Degree of C_8H_{17} modification (mol ±2%)	Distribution of C_8H_{17}	Mw (Da)	Ip
A8-35R	AP128-28R	A8-35	Acrylate	28	Random	14 000	1.60
A12-60R	AP107-27R	MB01	Methacrylate	27	Random	13 200	1.08
A12-80R	AP107-20R	MB02	Methacrylate	20	Random	13500	1.08
A12-80B	AP107-20B	MB07	Methacrylate	20	Multiblock	13600	1.08
A12-80B1	AP115-20B	APB49	Methacrylate	20	Multiblock	14500	1.70
A12-80B2	AP115-23B	MB06	Methacrylate	23	Multiblock	13600	1.70

A8-35R has been described as A8-35, the most used APol in previous membrane proteins papers. Both A8-35R and A12-60R contain isopropyl side groups in addition to c.a. 27% octyl side groups, but A8-60R is less polydisperse than A8-35R; A12-20R and A12-80B1 have been described as AP107-20R and AP115-20B, respectively (chemical names are from Ref. [20]). A12-80B1 and A12-80B2 (same Ip) are two batches obtained from the same parent polymer; A12-80B is synthesized from a parent polymer chain obtained by ATRP (see experimental procedures), and is therefore less polydisperse than A12-80B1 and A12-80B2. Mw is the weight averaged molecular weight of the final product (sodium salt). Ip is the polydispersity index (Mw/Mn, where Mn is the number averaged molecular weight).

Holey carbon-coated copper grids were rendered electrostatic by glow discharge prior to use. Samples at 0.2 mg/mL APol in 20 mM NaCl were first deposited on the holey carbon grid and flash frozen in liquid ethane cooled to −180 °C with liquid nitrogen. Typically, a 10 μL drop of sample was applied to the grid for a few seconds, the excess solution was blotted away with a filter paper, and the grid was rapidly frozen in liquid ethane. Vitrified samples were transferred into the microscope using a cryo-specimen holder maintained at −180 °C (Model 626, Gatan, Pleasanton). Images were recorded under low dose conditions with a Peltier cooled slow scan 1024×1024 pixels CCD camera (Model 794, Gatan, Pleasanton).

For TEM using negative staining, a 10 μL droplet of the sample solution was deposited on a glow discharged carbon coated grid for a few seconds, then negatively stained by replacing the sample solution with one or two drops of 2% (w/v) uranyl acetate. The excess of uranyl acetate was removed with a filter paper after 30 s incubation, and the grid was air dried before observation in the electron microscope.

2.3. Caleosin and oleosins cloning, expression and purification

Cloning, bacterial expression and purification as N-terminal 6His tag fusion proteins have been described for caleosin (Clo1 isoform: [23]) and oleosins S3 and S5 [12]. Briefly, purification was performed using a procedure based on affinity of the poly-histidine tail of the protein for a resin containing nickel (Ni Sepharose 6 Fast Flow, Amersham Biosciences), under denaturing conditions (8 M urea). We slightly modified the purification procedure by eluting proteins with 500 mM imidazole in the same buffer (100 mM sodium phosphate with 10 mM Tris pH 8.0). Clo, S3 and S5 final concentrations were within 0.5–2 g/L.

2.4. Solubility of proteins in amphipols or detergents

To investigate the ability of detergents and APols to maintain Clo and oleosins soluble in water-based buffers, stock solutions of proteins (1 g/L) in urea were supplemented with an excess of the amphiphilic molecules (5:1 to 20:1 g/g for APols, 1:1 to 250:1 g/g for detergents). After 15 mn incubation, samples were diluted 10-fold in a 20 mM Tris, 100 mM NaCl buffer pH 8.0 without urea. When using detergents, the corresponding amount of detergent was added in this diluting buffer. Absorbance spectra measured after dilutions followed by ultracentrifugation at 200000 *g* (TL 100 Ultracentrifuge, Beckman) gave the degree of solubility in the supernatant.

2.5. Samples preparation

Tris buffers were obtained from Tris–HCl/Tris-base mixture.

– APols in solution: except for dynamic light scattering (DLS) preparations, stock solutions of APol were prepared at 10% (w/v) in pure water and then diluted in 100 mM NaCl, 10–50 mM Tris buffer pH 8.0. Samples were ultracentrifuged (15 min, 200 000 *g*, 15 °C) before measurements.

– Proteins in SDS or APol: for large scale sample preparation (DLS, SRCD, Small-angle X-ray scattering: SAXS), proteins in 8 M urea eluting buffer were first incubated 15 mn with 2% SDS or 5 g of APol/g of protein. They were then 3-fold diluted in 10–50 mM Tris pH 8.0 buffer, 100 mM NaCl (or NaF for SRCD, see below), with 2% SDS (without in the case of APol trapping) to avoid chaotropic effect of urea. Finally, urea was removed by overnight dialysis (Slide-A-Lyzer 3.5 kDa cut-off cassettes, Pierce) against the same buffer. For SAXS and DLS, all samples and corresponding buffers were ultracentrifuged (15 min, 200 000 *g*, 15 °C) before measurements. For Clo samples in surfactants, solutions were supplemented with 50 mM DTT, and with 2 mM EDTA in order to avoid calcium-induced protein oligomerization.

2.6. Dynamic light scattering

Dynamic laser light scattering was performed with two instruments. Firstly, we used an ALV/CGS-3 compact goniometer system equipped with an ALV/LSE-5003 light scattering electronic and multiple τ digital correlator and a JDS Uniphase helium–neon laser. The output power was 22 mW, supplying vertically polarized light with a wavelength of 632.8 nm. The data were collected by monitoring the scattered light intensity at 90° and 140°, at 25 °C. Data were analyzed using the ALV-Correlator software version 3.0 and ALV-Fit & Plot Software provided by the manufacturer. Secondly, we used an HPPS Malvern instrument equipped with a 3.0 mW helium–neon laser also emitting at 632.8 nm. Measurements were carried out at 20 °C and 173° of the incident beam. Data were treated with DTS software 3.32. APols in powder were resuspended at 0.5% w/v (0.1% for A12-80B1) in 100 mM NaCl, 20 mM Tris buffer pH 8.0. Prior to measurements and after at least 3 h of incubation in this buffer, samples were ultracentrifuged and filtrated (0.22 μm).

2.7. Small angle X-ray scattering

For measurements performed at Soleil synchrotron (SWING beamline, Gif-sur-Yvette, France), sample-detector distance was 2.085 m, beamline energy was 9030 eV, sample exposure was 10 s. These settings allowed a Q range from 5 10^{-4} to 3 10^{-1} $Å^{-1}$. The Guinier plots represent the logarithm of the scattered intensity, I, as a function of the square of the scattering vector, Q ($Å^{-1}$). The Guinier approximation was used in a Q×Rg range from 0.5 to 1.5 to determine the radius of gyration of scattering particles [24]. Similar settings were used on I711 beamline at Max-lab synchrotron, Lund, Sweden, for measurements of the sample of A12-80B1 alone. A12-80B1 sample was prepared in 100 mM NaCl, 1 mM EDTA, 50 mM Tris buffer pH 8.0 at 1% (w/w) final concentration. A8-35R and A12-80B2 were prepared at the same concentration in 100 mM NaCl, 5% v/v glycerol, 20 mM

Tris buffer pH 8.0. Protein concentrations were 1.55 g/L in APol and 2.10 g/L in SDS.

2.8. Synchrotron radiation circular dichroism

Measurements were carried out at the Central Laboratory of the Research Councils (CLRC) on CD12 beamline, at Daresbury (UK), on UV1 beamline at the Institute for Storage Ring Facilities (ISA), in Aarhus (DK), and on DISCO beamline [25] at Soleil synchrotron (Gif-sur-Yvette, France). Standard Suprasil cells of 100 μm or 35 μm pathlength and Calcium Fluoride circular cuvettes (Hellma) [26] of 2.5 to 15 μm were used. The obtained spectra were scaled and superimposed for cross evaluation between different types of cells. Protein concentrations (determined using absorbance at 280 nm) ranged from 0.5 to 1 g/L. All samples were equilibrated overnight against their buffer (APol or protein-APol particles are not able to cross the 3.5 kDa MWCO dialysis membrane used). Three measurements for each protein concentration, from 170 to 280 nm with 1 nm intervals per second, were performed. Three consecutive scans of the baseline (using the dialysate) were obtained in the same manner. For all proteins, we used 10 mM Tris buffer pH 8.0 with 70 mM NaF in order to avoid absorbance from Cl ions otherwise used. Positioning of the detector within 5 mm of the sample reduced loss of signal due to scattered light.

For data processing, spectra of dialysis buffer were subtracted from those of corresponding samples. The 260–270 nm region was set to zero, and the resulting spectra were calibrated with CSA (D-10-camphorsulfonic acid) using the CDtool software [27]. For protein/APol samples, secondary structure determination was performed on spectra substracted either from that of the dialysed buffer or from that of an APol sample: in both cases the same results were obtained. Secondary structure determination was performed using ContinLL program in Dichroweb [28]. The reference set used was SP175 [29], which contains the largest set (72) of proteins to date. Normalized root-mean square deviations (NRMSD) gave insight of the most accurate fit for each data. Secondary structures were grouped in four different types: helical, beta, turns and unordered.

3. Results

3.1. Amphipols maintain soluble both caleosin and S5 oleosin in aqueous solution

Recombinant forms of caleosin (Clo) and S5 oleosin (S5) purified in 8 M urea yield solutions transparent to the eye. Ultracentrifugation and titration of the supernatant (Fig. 2) show that 83 ± 11% of Clo and 65 ± 13% of S5 are under a soluble form (these percentages reflect the different hydrophoby of the two proteins). A ten-fold dilution of urea solutions in aqueous buffer triggers obvious aggregation, resulting in 85% to 95% protein loss after ultracentrifugation. Accordingly, values above 50% solubility should be considered as representative of efficient solubility, therefore suitable for structural studies. Anionic detergents such as sodium dodecyl sulfate (SDS) and laurylsarcosin (LS) highly solubilized the proteins. All APols also yielded high solubility, irrespective of their chemical structure. Neutral detergents (lauryl maltoside: LM, and 3-((3-cholamidopropyl)dimethylammonium)-1-propanesulfonate: CHAPS), which are generally considered as less denaturing than anionic detergents, were markedly less effective to maintain solubility. The concentrations used for LM and CHAPS were above the CMCs, with a high detergent to protein ratio (200–400 g/g, corresponding here to more than 2000 detergent moles per protein mole). Therefore, neutral detergents do not shield against hydrophobic attractions for two representative integral proteins of lipid bodies, and have not been used further in this work.

The solubility increased when increasing SDS (respectively APol) to protein ratio (Fig. 3). The minimum amount of SDS needed to reach a high solubility (3 to 10 g/g protein) corresponded to a final concentration just above the CMC (1.2 mM in the presence of 100–200 mM Na^+ [30]), which presumably reflects the formation of protein aggregates upon dissociation of the SDS micelles. The maximum plateau solubility was essentially reached above 1 g/g for APols. Adding more polymer did not improve the ~85% solubility for Clo (Fig. 3B) or 60% solubility for S5 (Fig. 3D), which are values comparable to the solubility measured in urea. As opposed to the SDS, for which concentration increase allows reaching 100% protein solubility, APols presumably do not dissolve the aggregates originally present in the urea solutions.

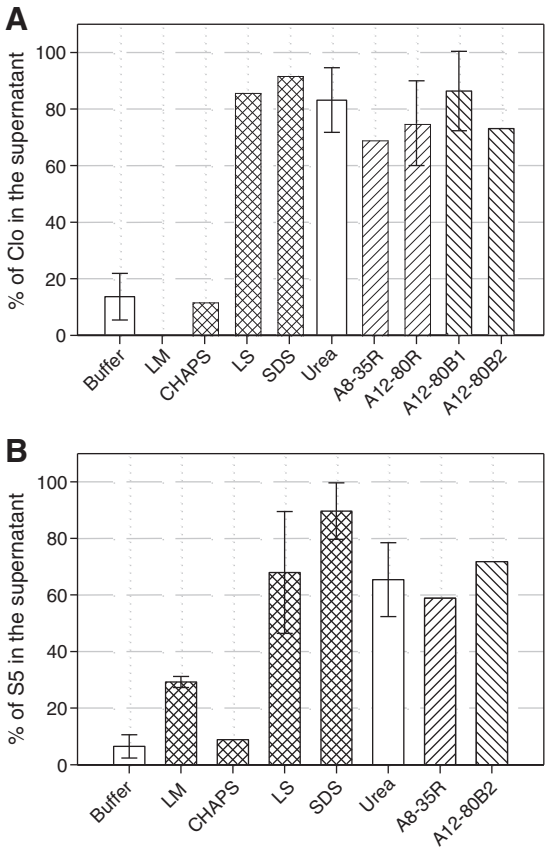

Fig. 2. Solubility of Clo (A) or S5 (B) in various surfactants. Proteins in 8 M urea were supplemented with surfactants, 10-fold diluted and ultracentrifuged. For both proteins, concentration was 0.1 g/L. (A) After dilution, final concentrations were: i) for detergents: LM, 0.30 g/L (0.60 mM); CHAPS, 20 g/L (33 mM); LS, 9.0 g/L (33 mM); SDS, 20 g/L (70 mM). ii) for APols: 0.5 g/L. Crossed boxes are for detergents, empty ones for conditions without surfactant. Ascending and descending hatched boxes are for random and blocky polymers respectively. (B) After dilution, final concentrations for detergents were 10 g/L (20 mM) for LM and 5.4 g/L (20 mM) for LS. All other concentrations for surfactants were identical to those in A.

To summarize, Clo and S5 are efficiently maintained in solution with three categories of surfactants: charged detergents SDS and LS, random APols and blocky ones. For S3 oleosin, SDS (91% solubility) and to a lesser extent A12-60R (47%) efficiently solubilized the protein (data not shown).

SDS assembles in solution to form micelles of ~2 nm radius [31]. Self-assembly of random APols has been extensively studied, indicating that they form particles of ~3 nm hydrodynamic radius (Rh) [32]. For recently developed blocky APols, self-assembly has also been studied, using at first only static and dynamic light scattering, suggesting that they form significantly larger particles of ~13 nm Rh [20]. In order to better understand the size and formation of protein–APols complexes, we further investigated blocky APols using complementary techniques, namely DLS, small angle X-ray scattering and transmission electron microscopy.

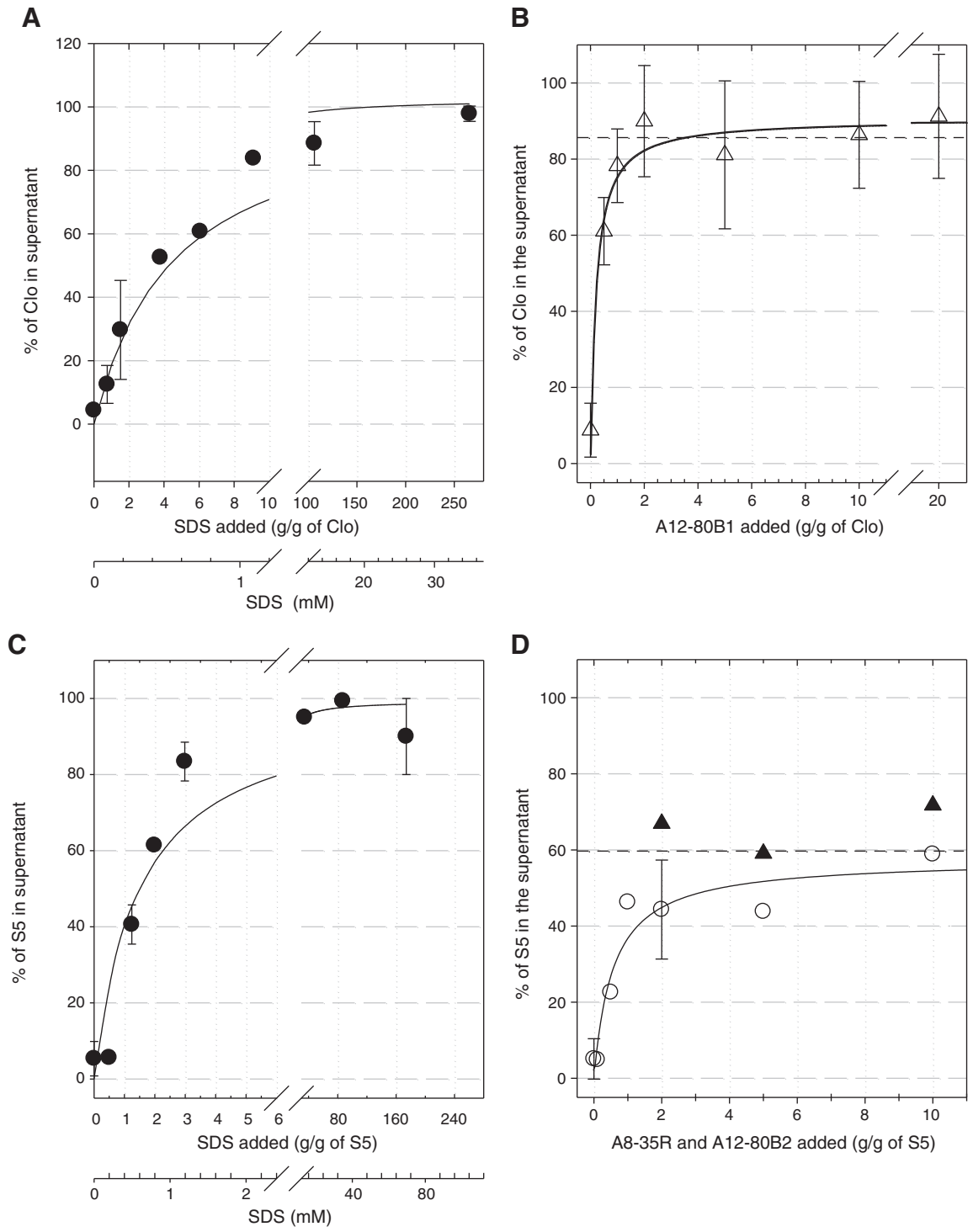

Fig. 3. Impact of SDS or amphipol amount on the solubility of Clo (A–B) or S5 (C–D). To allow comparison of SDS amounts with those of APols, in A and C, a double horizontal axis is shown: the SDS weight/protein weight, and a more usual mM scale. In B and D, horizontal bold dashed lines indicate the percent of protein maintained in solution in the presence of 8 M urea, namely 84% for Clo and 60% for S5. In D, open circles stand for S5/A8-35R (random) complexes whereas dark triangles are for S5/A12-80B2 (blocky) ones. Lines in all panels are tendencies obtained using a Michaelis–Menten like equation to determine a plateau value. Fits were determined using least squares method with Sigmaplot program.

3.2. Random and blocky polymers self-assemble in particles of different sizes in aqueous solution

Because a broad size distribution of the polymer micelles typically results in broad size distribution of their complexes with membrane proteins, good control of the size of these assemblies appears very important [33]. As indicated by DLS (Fig. 4), both random (A8-35R, A12-80R) and blocky polymers having hydrophobes gathered as small blocks (A12-80B, A12-80B1) form well-defined assemblies in water. Their size distributions were not sensitive to experimental scattering angle (90° or 140°), which points to the predominant contribution of particles having radii below 100–200 nm. Size distribution obtained with the random copolymers corresponds primarily to small objects having radii below 4 nm. Trace amount of aggregates (Rh>40 nm) were present in solutions of the random A12-80R. They can be removed by ultracentrifugation. In the same concentration conditions,

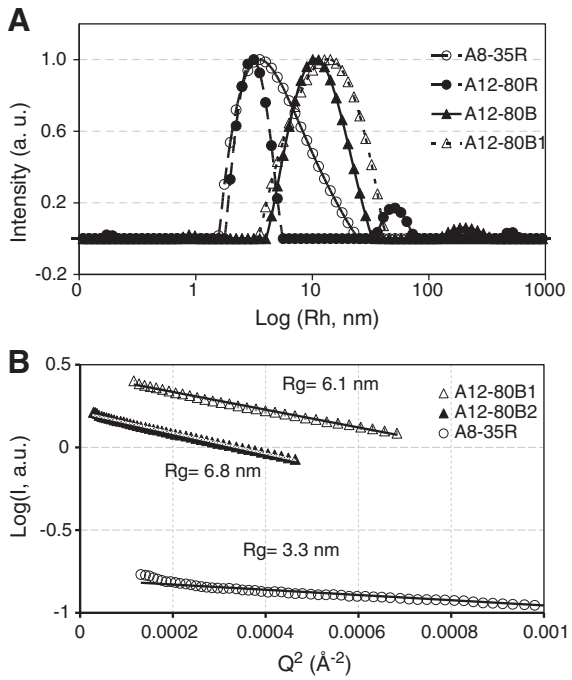

Fig. 4. Size dispersion of amphipols in aqueous solution. (A) Comparison of the intensity distribution obtained by DLS for random (circles) vs blocky (triangles) APols. (B) Comparison of the gyration radii obtained by SAXS experiments (Guinier plots of the intensities) for random (A8-35R) vs blocky (A12-80B1 and A12-80B2) APols.

the larger radii observed with the blocky polymers indicate a considerable increase of the molar mass of polymer self-assemblies. A narrow distribution was achieved (no aggregates, single peak at 10–14 nm and peak half-width about 5 nm) with no need for ultracentrifugation. The present DLS results are consistent with the previous studies of the average aggregation numbers by static light scattering (namely self-association of 10–15 chains for blocky polymers, and for random ones aggregation number ≤ 4). In other words, blocky APols form particles with a high number of hydrophobic chains (up to 400 octyl groups) as compared to random ones (less than 50 octyl groups) [20].

Guinier plots obtained from small angle X-ray scattering experiments (Fig 4B) indicate the existence in solution of small objects (radius of gyration Rg ~3.3 nm) for the random APol A8-35R, and of significantly larger objects (Rg 6–7 nm) for blocky APols.

The large size of micelles for blocky APols was confirmed by transmission electron microscopy (TEM) pictures. In the case of the random APol A12-80R, micrographs of polymers observed in negative stain show objects too small for accurate size distribution determination. Fig. 5A shows micrographs of A12-80B particles. The corresponding average radius (Rapp, calculated from measured apparent diameter) is 7.2 nm. However, staining by uranylacetate lowers the pH, which likely triggers the aggregation of neutralized polyacrylic acid chains. The high Rapp value observed could be attributable to possible aggregation on the grid, and may not reflect the size in solution. CryoTEM allows the direct observation of a suspension of polymers in an aqueous medium, in a frozen hydrated state (Fig. 5B and C). Fig. 5D shows the histogram of size distribution from measurements of 60 objects. The corresponding Rapp is 5.2 nm for A12-80B1, and 5.3 nm for A12-80B. Owing to the limited statistic achievable here by cryoTEM, this result pointed primarily the fact that we observe significantly larger assemblies with blocky APols than with random ones. In addition, these objects appeared essentially spherical and homogeneous (no internal structure could be distinguished).

Whatever method is used, the blocky nature of the APol markedly affects the size of the polymer micelles. This enables us to compare APols forming either small (Rh ~3.5 nm) or large (Rh ~12 nm) assemblies as regards to their capacity to solubilize lipid bodies IMPs.

3.3. Protein/amphipol complexes have a low polydispersity and their size depends on polymer grafting

In the absence of surfactant, previous DLS experiments on a caleosin suspension in aqueous solution showed the presence of large particles (Rh 50 to 250 nm), thus reflecting a high polydispersity of the preparation; particles with Rh corresponding to monomers within nanometer range were not detected [9]. Similar observations were done for oleosins [34].

In contrast, for the APols/proteins complexes, DLS (Fig. 6A) showed a relatively homogeneous size distribution. Within the experimental error, the size of protein–blocky APols complexes (10.1 and 11.4 nm) was essentially the same as that without protein (10.7 and 13.5 nm). For the random APol A8-35R, the Rh of the complex with S5 (7 nm) was significantly larger than that of APols micelles in the absence of protein (3.5 nm, see Fig. 4), and higher than that of S5–SDS micelles (4.7 nm). Accordingly, SAXS experiments on Clo-surfactant complexes indicate a significantly higher radius with the blocky APol A12-80B2 than with SDS. Table 2 summarizes all the radii obtained by different methods. As expected, Rh values, which takes into account both solvent and eventual shape effects, have higher values than Rg ones.

3.4. Caleosin and oleosins contain more β secondary structures in amphipols than in SDS

SRCD was performed to obtain data on secondary structures of the proteins in an aqueous environment containing detergents or APols. Amphipols used in this section were selected for their solubilization efficiency (see Fig. 2; A12-60R maintained 68% of Clo in solution, not shown). In our conditions, APols do not interfere with the circular dichroism signal from the proteins (see experimental section). Spectra could be recorded down to the vacuum UV (VUV) region (175 or 185 nm, depending on samples), and secondary structure determination was calculated with NRMSD values ranging from 0.05 to 0.26.

All three proteins contained 60 to 70% of folded regions (α, β, turns). Clo contains mainly α-helical structure in SDS, while it contains mainly β structures in APol (Fig. 7B). This difference is mainly due to a conversion of helical to β structure, as there is no significant increase of unordered structure in APol environment. Thus, Clo exists under two clearly distinct folds in SDS and APol environments. This feature, although less contrasted, is also true for oleosins. S3 oleosin is mainly α helical in SDS (41%), and contains comparable α and β contents (~25%) in A12-60R (Fig. 7D). In SDS, the shorter S5 oleosin has comparable α and β contents (~25%), whereas in APols it contains four times more β structures than α ones (Fig. 7F). For both Clo and S5, there is no significant difference in secondary structure content when comparing solutions containing random or blocky APols.

4. Discussion

The preparation of proteins under a soluble and folded form, and with low polydispersity in size, is an essential prerequisite for structural studies. These samples can be used either for characterization of protein solutions (DLS, SAXS), evaluation of the secondary structure content (SRCD), or high resolution structure determination (crystallography and nuclear magnetic resonance). Obtaining such solutions is especially demanding for IMPs from lipid bodies. We used S5, the most hydrophobic oleosin, S3, and caleosin, a less hydrophobic LB protein, to compare their solubilization by detergents and APols.

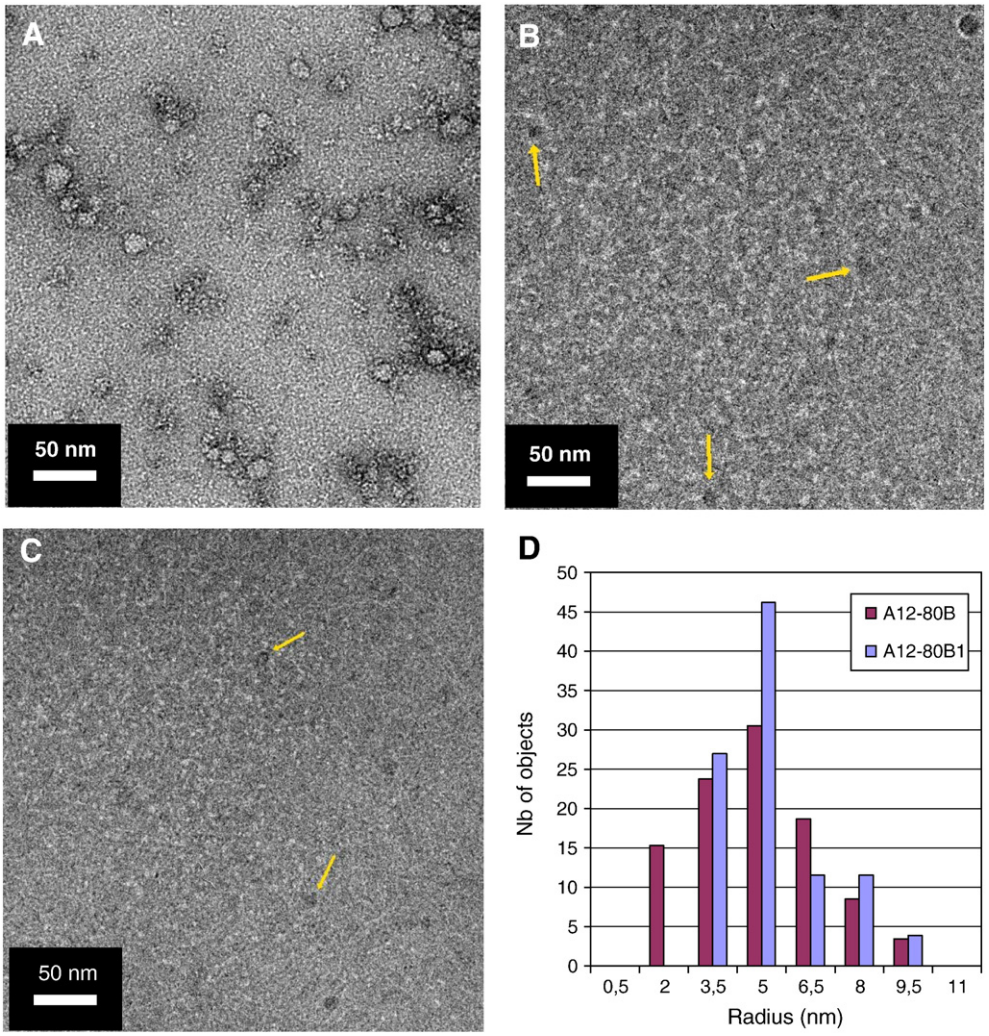

Fig. 5. Size of blocky amphipol particles evaluated by transmission electron microsocopy. (A) TEM of A12–80B using negative staining with uranylacetate. (B) Cryo-TEM of A12-80B. (C) Cryo-TEM of A12-80B1. (D) Comparison of the size range observed using cryo-TEM.

4.1. Amphipols appear to be suitable tools to maintain in solution hydrophobic proteins natively inserted in the phospholipid monolayer of lipid bodies

Few published studies report on the solubilizing efficiency of different surfactants on a given hydrophobic protein. In the case of oleosins, the first work using a defined criterion for solubility, i.e. centrifugation, was published recently [16]. However, the centrifugation conditions used (10 000 *g*) correspond typically to sedimentation conditions of subcellular organelles, but not of aggregated proteins. Here, we used markedly more severe criterions of solubility: ultracentrifugation conditions (200 000 *g*) able to pellet protein aggregates whose sedimentation coefficients are above ~32 Svedberg, which corresponds to an estimated molecular mass of ~1000 kDa. Moreover, our experiments were carried out in conditions close to biological ones, i.e. with 100 mM NaCl, and as far as possible without chaotropic additives (such as urea, thiourea or guanidinium chloride).

Anionic detergents (SDS and LS) maintain S5 oleosin and caleosin under a soluble form, but may denature proteins. In contrast, two representative milder detergents (LM and CHAPS) obviously failed with these proteins. They are known anyway to maintain the solubility of IMPs (as examples LM for cytochrome b_6 *f* [35], and CHAPS for nicotinic acetylcholin receptor [36]) and likely to preserve native states. Hydrophobic association between oleosin and neutral detergent is highly likely to occur, but could not prevent interprotein hydrophobic binding. Finally, all APols used in this study preserved a high solubility of IMPs from lipid bodies and low radii (i.e. below 20 nm) of the IMP–APol complexes.

In order to get insight into the importance of the size and composition of APols on oleosin solubility and polydispersity, we compared conventional random APols with multiblock copolymers specifically designed to display stronger hydrophobic binding. Both random and blocky APols form well-defined particles with proteins. The hydrodynamic radius of blocky polymers was not affected by the presence of protein, whereas for random polymers protein–APol radii were larger than those of free APol particles. This could reflect the fact that the radius change induced by protein binding is measurable for smaller particles (random polymers) and not for larger ones (blocky polymers).

Using the values of Clo/A12-80B1 and Clo/A12-80B2, the Rh/Rg ratio of the protein/APol complex is 1.33, which is very close to the theoretical one of 1.29 for the spherical particles [37]. Within experimental error, it suggests that these complexes are spherical objects. Such a behaviour was already described for bacteriorhodopsin/random APol complex [24]. In contrast, the particles of blocky APols alone give higher Rh/Rg (1.6 for A12-80B, 2.2 for A12-80B1). This has already been described [20], and could be related to a more compact character of random polymers particles, as compared to blocky polymer ones containing a peripheral crown of low density hydrophilic extensions. The sphericity of protein/blocky APol complex

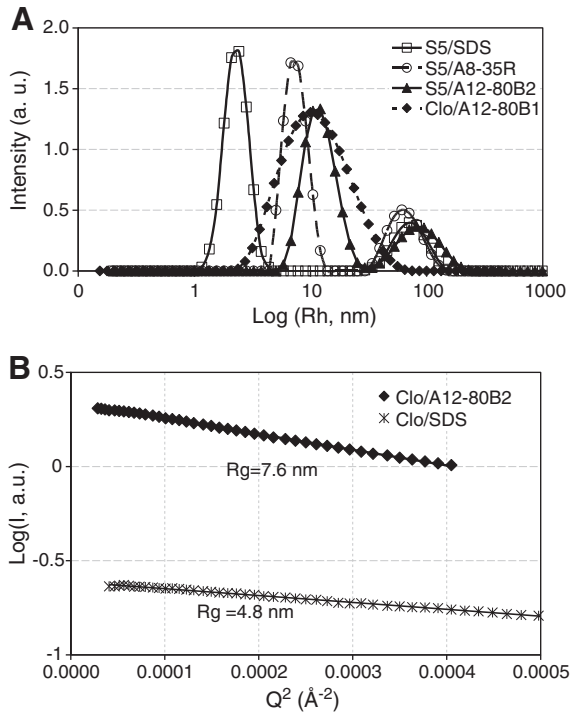

Fig. 6. Size dispersion of protein–surfactant complexes. (A) Comparison of the intensity distribution obtained by DLS for SDS, the random APol A8-35R with S5, or blocky APols with S5 or caleosin. A. U., arbitrary units. (B) Radii of gyration obtained by SAXS experiments (Guinier plots of the intensities) for caleosin in complex with the blocky APol A12-80B2 or with the SDS detergent.

could reflect a more compact assembly than is the case for the particles of blocky APols alone.

4.2. Synchrotron radiation circular dichroism contribution to the study of lipid bodies protein folding

The structural data on oleosins secondary structure are still scarce and contradictory [38]. For instance, the oleosin hydrophobic central region has been described either as predominantly α helical (using Fourier transform infrared, FTIR, on purified oil bodies: [39]), or as a predominantly β structure (FTIR on artificial oil bodies and CD on liposomes: [40]). Similarly, studies on full-length purified oleosins in Tris buffer gave contradictory results, with either a majority of β content (CD and FTIR: [41]), or of α content (CD: [42]). Less is known about caleosin. Its secondary structure has been studied in the presence of various aliphatic alcohols [23], suggesting that the polarity of the solvent influences mainly the α helical content.

CD is more adapted than FTIR to study the secondary structure of proteins in aqueous solution. CD is especially useful for the structural studies of membrane proteins, which are notoriously difficult to crystallize and are generally not suitable for NMR due to their low solubility, and to the large size of the protein-detergent micelles. However, caution has to be applied for the secondary structure determination using conventional CD. Firstly, β structures determination is less accurate because their CD spectra have poor amplitudes. The light sources of SRCD facilities provide a very high flux, improving the signal-to-noise ratio, and make the VUV region down to 170 nm accessible, increasing the information content obtainable from the spectra. Therefore secondary structure prediction is improved; e.g. β sheet content is more reliably predicted [43]. Secondly, up to now only soluble proteins are available as references, and the spectral peak positions of membrane proteins may be modified due to the different dielectric constants of the membrane environment relative to that of water [44].

In this work we used amphipols or the anionic detergent SDS. The latter clearly increases the helical content. SDS is known to favour α helices [45]. In APols (either random or blocky), the β sheets/α helices ratio was markedly increased for all Clo, S3 and S5 proteins. In the case of the apolipoprotein B-100 from human low density lipoproteins, there are evidences that the hydrophobic sides of the amphipathic β-sheets are in direct contact with the lipid core, and play a role in its organization [46]. Here we show that APols favour an increase of the β content of oleosins: it can be hypothesized that APols orient these particular membrane proteins in a more physiological state than the classical detergents. Such behaviour of APols vs detergents has been suggested for other membrane proteins [47].

Table 2
Experimental values of the radius determined for different particles.

			Radii (nm) determined using		
			DLS (Rh)	SAXS (Rg)	Cryo-TEM
APols alone	Random	A8-35R	3.5	3.3	
		A12-80R	3.2		
	blocky	A12-80B	10.7	6.8	5.3
		A12-80B1	13.5	6.1	5.2
Protein/SDS		Clo/SDS		4.8	
		S5/SDS	4.7		
Protein/APols	Random	S5/A8-35R	7.0		
	blocky	Clo/A12-80B1	10.1		
		Clo/A12-80B2		7.6	
		S5/A12-80B2	11.4		

4.3. Plausible secondary structure models of Clo, S3 and S5 maintained in solution

Our SRCD results indicate both α and β secondary structures for these three triblock proteins. What can be proposed for the secondary structure of their N-terminal, central hydrophobic, and C-terminal regions?

Considering the high-resolution structures known for more than 200 unique membrane proteins, the transmembrane-helix bundle appears as the fundamental motif of the plasma membrane proteins, whereas bacterial, mitochondrial and chloroplast outer-membrane proteins generally have a β-barrel motif [48]. Thus, the regions inserted in the phospholipid bilayer are generally all α helical, or rarely all β. Accordingly, it can be hypothesized that for Clo, S3 and S5 the secondary structure of the hydrophobic domain inserted in the phospholipid monolayer (and the underneath lipid core) is either all-α or all-β. SRCD results, either in SDS or in APols, indicate that S5 contains a high β content, and less α content as compared to Clo. In parallel, the central hydrophobic region represents around 50% of S5 residues, as opposed to only 17% for Clo. It therefore appears logical to propose that this hydrophobic domain is composed of β secondary structures for both proteins (Fig. 8). This is also proposed for S3, which central region shares 87% identity with that of S5. Such β structures could be more adapted to a neutral lipid environment than α helical structures, which induce a dipole with significant charges at each end of the helix. Secondary structure predictions using three different programs (in Phyre: [49]) propose essentially α helices for S3 and S5, a suggestion refuted by experimental SRCD results. However, the only program (JNet: [50]) among the three used that predicts some β-strands locates them in the central region (residues 78–80, close to the proline knot, for S3; residues 54–57, 61–66, close to the proline knot, and 83–85 for S5). In addition, the more recent I-TASSER software [51] proposes one β strand in the central region for both S3 (residues 55–60) and S5 (residues 39–44). For Clo, a β strand is predicted by all four programs in the central hydrophobic region (127–131), close to the proline knot, which has been suggested to connect β-strands [52]. These predictions are in accordance with our proposal.

What can be proposed for the C- and N-terminal hydrophilic regions? For S5, assuming that the central region contains β secondary structures, they should contain α helices. In accordance, as compared to S5, the higher α content observed for S3 is attributable to its longer

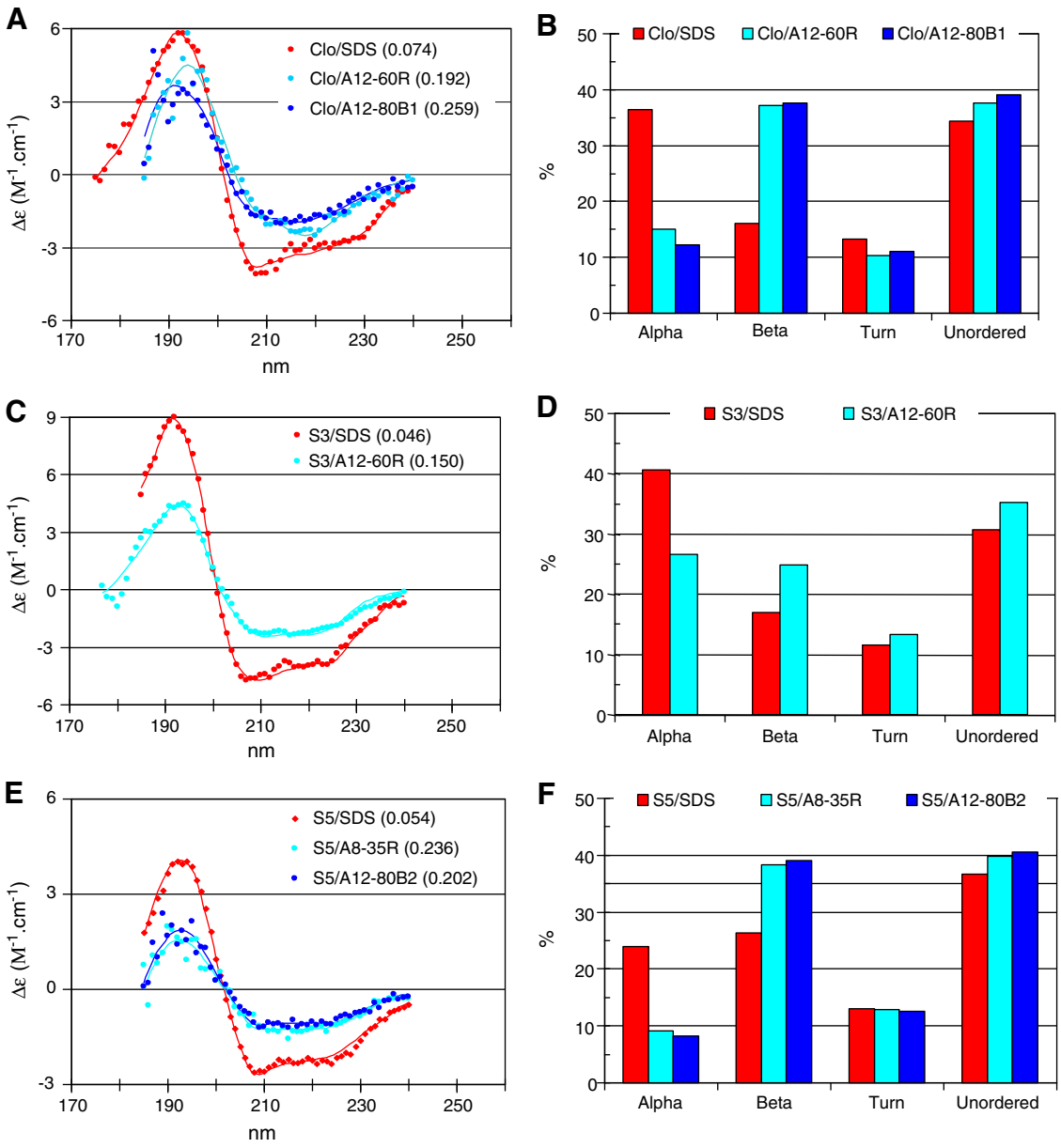

Fig. 7. Synchrotron radiation circular dichroism on Clo, S3 or S5. (A–C–E) Dichroic signals of Clo (A), S3 (C), and S5 (E) in SDS or in APols. Red curves and symbols are for SDS solutions, cyan ones for the random APols A8-35R or A12-60R, and blue ones for the blocky APols A12-80B1 or A12-80B2. Continuous lines show the curves reconstituted using the secondary structure content estimated by Dichroweb program. Normalized root-mean square deviations are given in parentheses. (B–D–F) Secondary structure contents of the proteins maintained in solution by SDS or various APols.

N-terminal and C-terminal regions. It is noticeable that the known crystal structures of N- and C-terminal domains of lipid bodies IMPs contain mainly α helices (for instance the N-terminal domain of apolipoprotein E [53], and the C-terminal domain of TIP47 [54]). For Clo, the β content indicated by SRCD in APols is obviously too high (~37%) to be entirely included in the central hydrophobic region, therefore the terminal regions must contain β-strands. There is no obvious indication for the position of α and β structures, except for the calcium-binding domain (including residues 75–86). It has been described for many soluble proteins as a helix–loop–helix motif; therefore α helices should be present in the N-terminal domain, close to the central hydrophobic region.

5. Conclusions

APols, in addition to their known capacity to maintain IMPs soluble, can maintain in solution a new class of very hydrophobic proteins, designed by evolution to be inserted into a phospholipid monolayer. This solubilization is achieved with a low dispersity and a specific fold. The amount (g/g) of APol needed to achieve maximum solubility of S5 oleosin or Clo is lower than that of SDS or LS (the only detergents improving solubility in our hands). Accordingly, APols appear to be promising molecules for structural studies of oleosins and the set of APols available (random, multiblock, with or without isopropyl side group, etc.) opens the route to fine tuning of their effect on solubility, folding, and stability. Despite the difference in their average hydrodynamic radii, at this stage our study does not point to any clear advantage of using multiblock instead of random APols. However, the impact of random vs blocky APols on the stability of folded structures deserves future complementary investigations.

In accordance with SRCD results, we propose a model with β secondary structures in the central hydrophobic region of the triblock LB proteins Clo, S3 and S5. So far, few β-barrel membrane proteins inserted in phospholipids bilayers have been crystallized [55], and none of them in

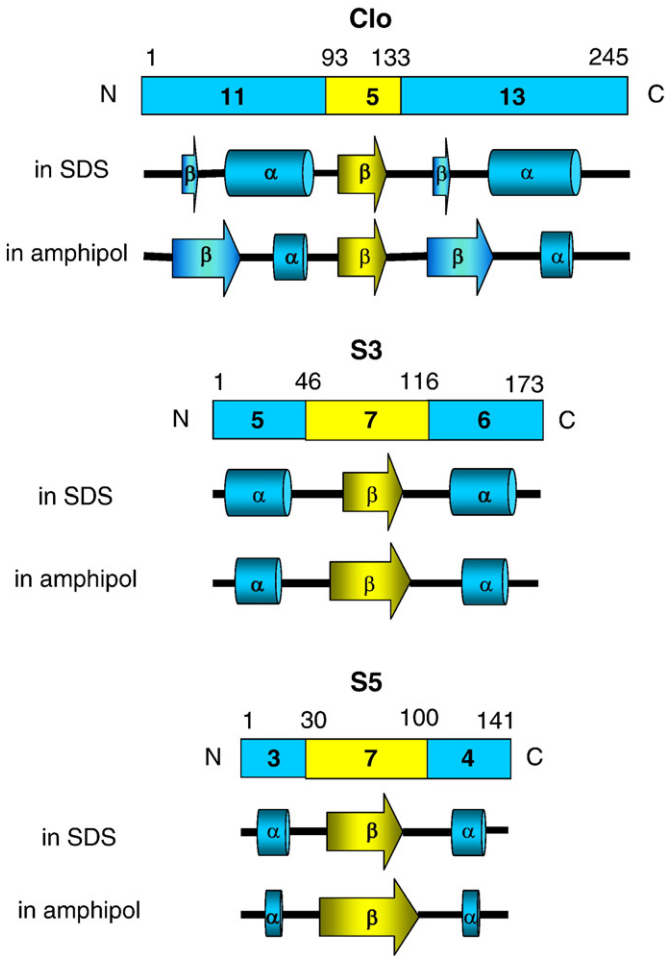

Fig. 8. Proposed models of Clo, S3 or S5 in different surfactants. Rectangles (upper parts) remind the known triblock sequences of Clo and oleosins: the central hydrophobic domain is yellow, and the N- and C-terminal hydrophilic domains are blue; lengths are proportional to the MW (labeled) of each domain in kDa. Residue numbers are indicated over the rectangles. Cylinders indicate α-helical domains and arrows β domains. Domains length is proportional to their molecular weight (same scale as rectangles) according to the secondary structure percents from SRCD. Turns and unordered structures are indicated by dark thick lines.

eukaryotic cells (with the exception of proteins inserted in mitochondrial or chloroplast outer membrane, which are evolutionary related to bacterial proteins). For IMPs from lipid bodies, a majority of the known crystal or NMR structures contain α helices. Although rare, β-strands are described in some lipoproteins, like lamprey lipovitellin [56] or human apolipoprotein D [57]. Our results suggest that oleosins could be an original example of eukaryotic integral membrane proteins inserted through β strands into the phospholipid monolayer of plant lipid bodies.

Acknowledgements

We thank Javier Perez, SWING beamline from Soleil synchrotron, and the staff from Astrid beamline, Aarhus synchrotron, for precious help during SAXS and SRCD experiments, and Roger Liu for helpful discussion on polymer analysis. This work was supported by grants from ParisTech PostDoctoral fellowship (YG), the Centre National de la Recherche Scientifique (UMR 7615), Soleil synchrotron, and ANR-08-CP2D-19-01 (SOPOL project).

References

[1] J.P. Overington, B. Al-Lazikani, A.L. Hopkins, How many drug targets are there? Nat. Rev. Drug Discov. 5 (2006) 993–996.
[2] V. Leduc, D.A. Moneret-Vautrin, J.T. Tzen, M. Morisset, L. Guerin, G. Kanny, Identification of oleosins as major allergens in sesame seed allergic patients, Allergy 61 (2006) 349–356.
[3] P. Jolivet, E. Roux, S. D'Andrea, M. Davanture, L. Negroni, M. Zivy, T. Chardot, Protein composition of oil bodies in *Arabidopsis thaliana* ecotype WS, Plant Physiol. Biochem. 42 (2004) 501–509.
[4] H. Næsted, G.I. Frandsen, G.-Y. Jauh, I. Hernandez-Pinzon, H.B. Nielsen, D.J. Murphy, J.C. Rogers, J. Mundy, Caleosins: Ca^{2+}-binding proteins associated with lipid bodies, Plant Mol. Biol. 44 (2000) 463–476.
[5] L.J. Lin, S.S. Tai, C.C. Peng, J.T. Tzen, Steroleosin, a sterol-binding dehydrogenase in seed oil bodies, Plant Physiol. 128 (2002) 1200–1211.
[6] P.J. Eastmond, SUGAR-DEPENDENT1 encodes a patatin domain triacylglycerol lipase that initiates storage oil breakdown in germinating *Arabidopsis* seeds, Plant Cell 18 (2006) 665–675.
[7] R.M. Siloto, K. Findlay, A. Lopez-Villalobos, E.C. Yeung, C.L. Nykiforuk, M.M. Moloney, The accumulation of oleosins determines the size of seed oilbodies in *Arabidopsis*, Plant Cell 18 (2006) 1961–1974.
[8] B.M. Abell, L.A. Holbrook, M. Abenes, D.J. Murphy, M.J. Hills, M.M. Moloney, Role of the proline knot motif in oleosin endoplasmic reticulum topology and oil body targeting, Plant Cell 9 (1997) 1481–1493.
[9] Z. Purkrtova, Expression, purification and characterisation of structural and functional properties of caleosin from *A. thaliana*, PhD thesis, Thiverval-Grignon, Prague, 2007.
[10] A.A. Ajees, G.M. Anantharamaiah, V.K. Mishra, M.M. Hussain, H.M. Murthy, Crystal structure of human apolipoprotein A-I: insights into its protective effect against cardiovascular diseases, Proc. Natl. Acad. Sci. U. S. A. 103 (2006) 2126–2131.
[11] D. Fan, Y. Zheng, D. Yang, J. Wang, NMR solution structure and dynamics of an exchangeable apolipoprotein, *Locusta migratoria* apolipophorin III, J. Biol. Chem. 278 (2003) 21212–21220.
[12] S. D'Andrea, P. Jolivet, C. Boulard, C. Larre, M. Froissard, T. Chardot, Selective one-step extraction of *Arabidopsis thaliana* seed oleosins using organic solvents, J. Agric. Food Chem. 55 (2007) 10008–10015.
[13] M. Millichip, A.S. Tatham, F. Jackson, G. Griffiths, P.R. Shewry, A.K. Stobart, Purification and characterization of oil-bodies (oleosomes) and oil-body boundary proteins (oleosins) from the developing cotyledons of sunflower (*Helianthus annuus* L.), Biochem. J. 314 (Pt 1) (1996) 333–337.
[14] E. Roux, S. Baumberger, M.A. Axelos, T. Chardot, Oleosins of *Arabidopsis thaliana*: expression in *Escherichia coli*, purification, and functional properties, J. Agric. Food Chem. 52 (2004) 5245–5249.
[15] M. Li, J.S. Keddie, L.J. Smith, D.C. Clark, D.J. Murphy, Expression and characterization of the N-terminal domain of an oleosin protein from sunflower, J. Biol. Chem. 268 (1993) 17504–17512.
[16] H. Kim, S.-Y. Kim, N.S. Han, B.Y. Tao, Solubilization conditions for hydrophobic membrane protein, oleosin, in soybeans, Biotechnol. Bioprocess Eng. 12 (2007) 542–547.
[17] C. Tribet, R. Audebert, J.L. Popot, Amphipols: polymers that keep membrane proteins soluble in aqueous solutions, Proc. Natl. Acad. Sci. U. S. A. 93 (1996) 15047–15050.
[18] J.L. Popot, E.A. Berry, D. Charvolin, C. Creuzenet, C. Ebel, D.M. Engelman, M. Flotenmeyer, F. Giusti, Y. Gohon, Q. Hong, J.H. Lakey, K. Leonard, H.A. Shuman, P. Timmins, D.E. Warschawski, F. Zito, M. Zoonens, B. Pucci, C. Tribet, Amphipols: polymeric surfactants for membrane biology research, Cell. Mol. Life Sci. 60 (2003) 1559–1574.
[19] M. Zoonens, F. Giusti, F. Zito, J.L. Popot, Dynamics of membrane protein/amphipol association studied by Forster resonance energy transfer: implications for in vitro studies of amphipol-stabilized membrane proteins, Biochemistry 46 (2007) 10392–10404.
[20] R.C.W. Liu, A. Pallier, M. Brestaz, N. Pantoustier, C. Tribet, Impact of polymer microstructure on the self-assembly of amphiphilic polymers in aqueous solutions, Macromolecules 40 (2007) 4276–4286.
[21] L. Czerski, C.R. Sanders, Functionality of a membrane protein in bicelles, Anal. Biochem. 284 (2000) 327–333.
[22] C. Duval-Terrie, P. Cosette, G. Molle, G. Muller, E. De, Amphiphilic biopolymers (amphibiopols) as new surfactants for membrane protein solubilization, Protein Sci. 12 (2003) 681–689.
[23] Z. Purkrtova, S. d'Andrea, P. Jolivet, P. Lipovova, B. Kralova, M. Kodicek, T. Chardot, Structural properties of caleosin: a MS and CD study, Arch. Biochem. Biophys. 464 (2007) 335–343.
[24] Y. Gohon, T. Dahmane, R.W. Ruigrok, P. Schuck, D. Charvolin, F. Rappaport, P. Timmins, D.M. Engelman, C. Tribet, J.L. Popot, C. Ebel, Bacteriorhodopsin/amphipol complexes: structural and functional properties, Biophys. J. 94 (2008) 3523–3537.
[25] A. Giuliani, F. Jamme, V. Rouam, F. Wien, J.L. Giorgetta, B. Lagarde, O. Chubar, S. Bac, I. Yao, S. Rey, C. Herbeaux, J.L. Marlats, D. Zerbib, F. Polack, M. Refregiers, DISCO: a low-energy multipurpose beamline at synchrotron SOLEIL, J. Synchrotron Radiat. 16 (2009) 835–841.
[26] F. Wien, B.A. Wallace, Calcium fluoride micro cells for synchrotron radiation circular dichroism spectroscopy, Appl. Spectrosc. 59 (2005) 1109–1113.
[27] J. Lees, F. Smith, F. Wien, A. Miles, B. Wallace, CDtool — an integrated software package for circular dichroism spectroscopic data processing, analysis and archiving, Anal. Biochem. 322 (2004) 285–289.
[28] L. Whitmore, B.A. Wallace, DICHROWEB, an online server for protein secondary structure analyses from circular dichroism spectroscopic data, Nucleic Acids Res. 32 (2004) W668–W673.
[29] J. Lees, A. Miles, F. Wien, B. Wallace, A reference database for circular dichroism spectroscopy covering fold and secondary structure space, Bioinformatics 22 (2006) 1955–1962.

[30] M. Le Maire, P. Champeil, J.V. Moller, Interaction of membrane proteins and lipids with solubilizing detergents, Biochim. Biophys. Acta 1508 (2000) 86–111.
[31] A. Suárez Varela, M. Sández Macho, A. Gil González, The size of sodium dodecyl sulfate micelles in the presence ofn-alcohols as determined by fluorescence quenching measurements, Colloid Polym. Sci. 273 (1995) 876–880.
[32] Y. Gohon, F. Giusti, C. Prata, D. Charvolin, P. Timmins, C. Ebel, C. Tribet, J.L. Popot, Well-defined nanoparticles formed by hydrophobic assembly of a short and polydisperse random terpolymer, amphipol A8-35, Langmuir 22 (2006) 1281–1290.
[33] A.M. Seddon, P. Curnow, P.J. Booth, Membrane proteins, lipids and detergents: not just a soap opera, Biochim. Biophys. Acta 1666 (2004) 105–117.
[34] E. Roux, Les oléosines, de nouveaux émulsifiants d'origine végétale, PhD thesis, Paris 2003.
[35] D. Stroebel, Y. Choquet, J.L. Popot, D. Picot, An atypical haem in the cytochrome b6f complex, Nature 426 (2003) 413–418.
[36] K.L. Martinez, Y. Gohon, P.J. Corringer, C. Tribet, F. Merola, J.P. Changeux, J.L. Popot, Allosteric transitions of Torpedo acetylcholine receptor in lipids, detergent and amphipols: molecular interactions vs. physical constraints, FEBS Lett. 528 (2002) 251–256.
[37] O. Glatter, R. May, International tables for crystallography, vol. C, Springer, 2006.
[38] Z. Purkrtova, P. Jolivet, M. Miquel, T. Chardot, Structure and function of seed lipid body-associated proteins, C. R. Biol. 331 (2008) 746–754.
[39] D.J. Lacey, N. Wellner, F. Beaudoin, J.A. Napier, P.R. Shewry, Secondary structure of oleosins in oil bodies isolated from seeds of safflower (*Carthamus tinctorius* L.) and sunflower (*Helianthus annuus* L.), Biochem. J. 334 (1998) 469–477.
[40] M. Li, D.J. Murphy, K.H. Lee, R. Wilson, L.J. Smith, D.C. Clark, J.Y. Sung, Purification and structural characterization of the central hydrophobic domain of oleosin, J. Biol. Chem. 277 (2002) 37888–37895.
[41] M. Li, L.J. Smith, D.C. Clark, R. Wilson, D.J. Murphy, Secondary structures of a new class of lipid body proteins from oilseeds, J. Biol. Chem. 267 (1992) 8245–8253.
[42] L. Pons, C. Chery, N. Mrabet, H. Schohn, F. Lapicque, J.L. Gueant, Purification and cloning of two high molecular mass isoforms of peanut seed oleosin encoded by cDNAs of equal sizes, Plant Physiol. Biochem. 43 (2005) 659–668.
[43] A.J. Miles, B.A. Wallace, Synchrotron radiation circular dichroism spectroscopy of proteins and applications in structural and functional genomics, Chem. Soc. Rev. 35 (2006) 39–51.
[44] B.A. Wallace, J.G. Lees, A.J.W. Orry, A. Lobley, R.W. Janes, Analyses of circular dichroism spectra of membrane proteins, Protein Sci. 12 (2003) 875–884.
[45] S. Micelli, D. Meleleo, V. Picciarelli, M.G. Stoico, E. Gallucci, Effect of nanomolar concentrations of sodium dodecyl sulfate, a catalytic inductor of alpha-helices, on human calcitonin incorporation and channel formation in planar lipid membranes, Biophys. J. 87 (2004) 1065–1075.
[46] J.P. Segrest, M.K. Jones, H. De Loof, N. Dashti, Structure of apolipoprotein B-100 in low density lipoproteins, J. Lipid Res. 42 (2001) 1346–1367.
[47] C.L. Pocanschi, T. Dahmane, Y. Gohon, F. Rappaport, H.J. Apell, J.H. Kleinschmidt, J.L. Popot, Amphipathic polymers: tools to fold integral membrane proteins to their active form, Biochemistry 45 (2006) 13954–13961.
[48] S.H. White, Biophysical dissection of membrane proteins, Nature 459 (2009) 344–346.
[49] R.M. Bennett-Lovsey, A.D. Herbert, M.J. Sternberg, L.A. Kelley, Exploring the extremes of sequence/structure space with ensemble fold recognition in the program Phyre, Proteins 70 (2008) 611–625.
[50] C. Cole, J.D. Barber, G.J. Barton, The Jpred 3 secondary structure prediction server, Nucleic Acids Res. 36 (2008) W197–W201.
[51] A. Roy, A. Kucukural, Y. Zhang, I-TASSER: a unified platform for automated protein structure and function prediction, Nat. Protoc. 5 (2010) 725–738.
[52] J.C. Chen, C.C. Tsai, J.T. Tzen, Cloning and secondary structure analysis of caleosin, a unique calcium-binding protein in oil bodies of plant seeds, Plant Cell Physiol. 40 (1999) 1079–1086.
[53] C. Wilson, M.R. Wardell, K.H. Weisgraber, R.W. Mahley, D.A. Agard, Three-dimensional structure of the LDL receptor-binding domain of human apolipoprotein E, Science 252 (1991) 1817–1822.
[54] S.J. Hickenbottom, A.R. Kimmel, C. Londos, J.H. Hurley, Structure of a lipid droplet protein; the PAT family member TIP47, Structure 12 (2004) 1199–1207.
[55] M.M. Gromiha, M. Suwa, Current developments on beta-barrel membrane proteins: sequence and structure analysis, discrimination and prediction, Curr. Protein Pept. Sci. 8 (2007) 580–599.
[56] T.A. Anderson, D.G. Levitt, L.J. Banaszak, The structural basis of lipid interactions in lipovitellin, a soluble lipoprotein, Structure 6 (1998) 895–909.
[57] A. Eichinger, A. Nasreen, H.J. Kim, A. Skerra, Structural insight into the dual ligand specificity and mode of high density lipoprotein association of apolipoprotein D, J. Biol. Chem. 282 (2007) 31068–31075.